

Analytic Description of DGP Perturbations on All Scales

Sanjeev S. Seahra¹ and Wayne Hu²

¹*Department of Mathematics and Statistics, University of New Brunswick, Fredericton, NB, Canada E3B 5A3*

²*Department of Astronomy & Astrophysics, Kavli Institute for Cosmological Physics,
and Enrico Fermi Institute, The University of Chicago, Chicago, IL 60637-1433*

(Dated: November 20, 2018)

We develop analytic solutions for the linear evolution of metric perturbations in the DGP braneworld modified gravity scenario including near-horizon and superhorizon modes where solutions in the bulk are required. These solutions apply to both the self-accelerating and normal branch and elucidate the nature of coordinate singularities and initial data in the bulk as well as their effect on perturbation evolution on the brane. Even on superhorizon scales, the evolution of metric perturbations is no longer necessarily scale free due to multiple resonances in the bulk. Based on these analytic solutions, we devise convenient fitting functions for the evolution that bridge the various spatial and temporal regimes. Compared with a direct numerical integration of the bulk equations, the fits are accurate at the percent level and are sufficient for current and upcoming observational tests.

I. INTRODUCTION

The Dvali-Gabadadze-Porrati (DGP) model modifies General Relativity on large scales by positing that we live on a 4-dimensional brane in a 5-dimensional Minkowski bulk [1]. On scales larger than the crossover scale r_c , gravity becomes 5-dimensional and hence one can hope to uncover extra-dimensional physics by studying the evolution of density perturbations on scales approaching r_c . The DGP model has two branches of cosmological solutions [2]. On the self-accelerating branch, the expansion of the universe accelerates without a cosmological constant or dark energy. On the normal branch, brane tension is required to accelerate the expansion though gravity is still modified on large scales.

To solve for the evolution of perturbations on either branch near the horizon scale and beyond requires following metric perturbations into the bulk. On the self-accelerating branch approximate scaling solutions [3] showed that modifications near the horizon scale are in significant tension with the data from the cosmic microwave background [4, 5]. In this paper, we present the first quantitative and thorough comparison of these approximate solutions with direct numeric simulations [6]. We confirm that the scaling solutions used in [4, 5] are sufficiently accurate to expose tension between self-accelerating DGP and observations. It is also worthwhile noting that the pure de Sitter phase of the self-accelerating branch suffers from a perturbative ghost mode (see e.g. [7]), which is significant theoretical challenge for the model.

Numerical integration of the bulk metric equations have also been performed on the ghost-free normal branch [6]. In order to facilitate studies of cosmological constraints on the normal branch, it is useful to have a simple but accurate description of the evolution of perturbations in terms of the fundamental cosmological parameters and crossover scale. Scaling approaches on the normal branch have also been studied [8] but without a proper treatment of initial conditions in the bulk and boundary conditions on the brane.

In this paper, we employ analytic and numerical techniques to devise such a description. In fact, preliminary versions of results from this work have already been used to set cosmological constraints on the crossover scale on both branches of DGP [9].

We begin in §II with a brief review of the equations governing the background and perturbations on both the self-accelerating and normal branches of the DGP model. We outline the numerical methodology for obtaining solutions of the perturbation equations as well as the scaling ansatz that provides insight into their nature in §III. In §IV we combine scaling results with Green's function techniques to obtain analytic solutions in the matter and de Sitter epochs. We join these solutions into simple but accurate global descriptions of perturbation evolution via fitting functions in §V and discuss these results in §VI.

II. FORMALISM

We begin in §II A with a review of the DGP field equations and bulk geometry. In §II B-II C we apply the field equations to the background evolution and perturbation evolution respectively. We discuss the initial conditions and singularities in the bulk in §II D and the effective equations of motion on the brane in §II E.

A. Field Equations and Bulk Geometry

The action of the DGP model is

$$S = \frac{1}{2\kappa_5^2} \int_{\mathcal{M}} d^5 X \sqrt{-g} R^{(5)} + \frac{1}{2\kappa_4^2} \int_{\partial\mathcal{M}_b} d^4 x \sqrt{-\gamma} R^{(4)} + \int_{\partial\mathcal{M}_b} d^4 x \sqrt{-\gamma} (\mathcal{L}_m - \sigma). \quad (1)$$

Here, σ is the brane tension and \mathcal{L}_m is the matter Lagrangian. The field equations satisfied in the empty bulk are simply

$$R_{ab}^{(5)} = 0, \quad (2)$$

whereas those on the brane are given by [10, 11]

$$G_{\mu\nu}^{(4)} = (2\kappa_4^2 r_c)^2 \Pi_{\mu\nu} - \mathcal{E}_{\mu\nu}, \quad (3)$$

where

$$\begin{aligned} \Pi_{\mu\nu} &= -\frac{1}{4} \tilde{T}_{\mu\alpha} \tilde{T}_\nu{}^\alpha + \frac{1}{12} \tilde{T} \tilde{T}_{\mu\nu} + \frac{1}{24} (3 \tilde{T}_{\alpha\beta} \tilde{T}^{\alpha\beta} - \tilde{T}^2) g_{\mu\nu}, \\ \tilde{T}_{\mu\nu} &= T_{\mu\nu} - \sigma g_{\alpha\beta} - \kappa_4^{-2} G_{\mu\nu}^{(4)}, \end{aligned} \quad (4)$$

and $\mathcal{E}_{\mu\nu}$ is the trace-free projection of the 5-dimensional Weyl tensor. Here the crossover scale is defined by

$$r_c = \frac{\kappa_5^2}{2\kappa_4^2}. \quad (5)$$

The background metric or geometry converts the field equations into the modified Friedmann equation and imposes the distinction between the two branches of solutions. The background bulk metric can be expressed in terms of Gaussian normal (GN) coordinates (t, y, \mathbf{x}) [12]

$$ds^2 = -n^2(t, y) dt^2 + b^2(t, y) d\mathbf{x}^2 + dy^2, \quad (6)$$

or null coordinates (u, v, \mathbf{x}) ,

$$ds^2 = -du dv + r_c^{-2} v^2 d\mathbf{x}^2. \quad (7)$$

For the analytic solutions below, we employ GN coordinates whereas for the numerical characteristic integration (CI) we use null coordinates.

In GN coordinates the brane is always at $y = 0$, while in the null coordinates the brane is moving. The metric functions in the GN line element are

$$n(t, y) = 1 + \epsilon \left(H + \frac{\dot{H}}{H} \right) y, \quad b(t, y) = a(t) (1 + \epsilon H y), \quad (8)$$

where $\epsilon = +1$ on the self-accelerating branch and $\epsilon = -1$ on the normal branch. Here $H = \dot{a}/a$ is the Hubble parameter on the brane.

The coordinate transformation between the two systems is

$$u = \frac{1}{r_c} \left[\int_{a_0}^{a(t)} \frac{d\tilde{a}}{H^2(\tilde{a})\tilde{a}^2} - \frac{\epsilon y}{Ha} \right] + u_0, \quad v = r_c b(t, y), \quad (9)$$

where $u(a_0) = u_0$ is a constant defining the origin of the coordinate system at a_0 . Ignoring inflation and taking only matter components on the brane, we can take $a_0 \rightarrow 0$ and set $u_0 = 0$.

With these assumptions the coordinate transformation fixes the position of the brane in the null system:

$$u_b(t) = \frac{1}{r_c} \int_0^{a(t)} \frac{d\tilde{a}}{H^2(\tilde{a})\tilde{a}^2}, \quad v_b(t) = r_c a(t). \quad (10)$$

Note that both line elements have a coordinate singularity: either when $b(t, y) = 0$ or $v = 0$. These singularities are actually at the same place. The relationship between the two coordinate systems is illustrated in Fig. 1. Note that the $v = 0$ singularity is only accessible in the normal branch.

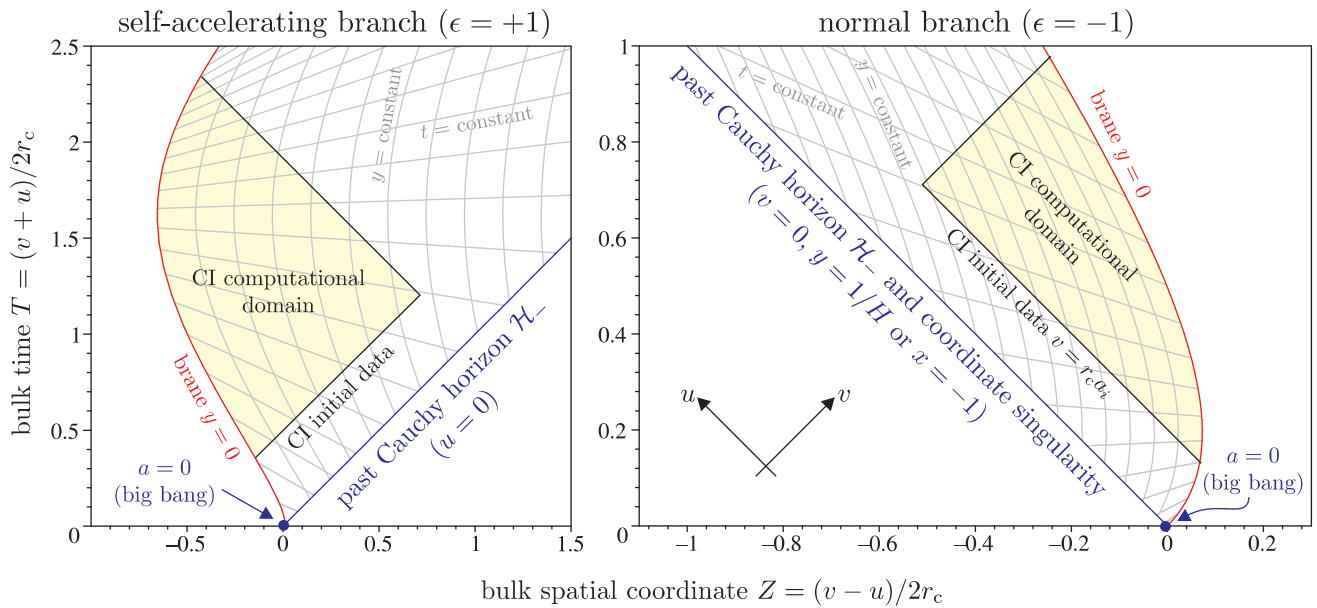


FIG. 1: Spacetime diagram of a brane trajectory through the bulk for the self-accelerating and normal branch. The grey timelike lines are the $y = \text{constant}$ traces of the Gaussian normal coordinate system, while the spacelike grey lines are the $t = \text{constant}$ traces. Lines of constant u and v are tilted at 45° and represent the trajectory of light rays in the bulk. The brane is at $y = 0$. In both cases there is a past Cauchy horizon \mathcal{H}_- in the bulk, and for the normal branch \mathcal{H}_- is coincident with a coordinate singularity. In this plot, we have chosen the constant u_0 in Eq. (9) such that the Cauchy horizon in the self-accelerating branch is at $u = 0$.

B. Background Evolution

The field equations in the spatially flat background reduce to

$$H = \frac{1}{2r_c} \left[\epsilon + \sqrt{1 + \frac{4}{3} \kappa_4^2 r_c^2 (\rho + \sigma)} \right], \quad (11)$$

with the bulk metric determined by H through Eqs. (8-10). If we further assume that the energy content of brane ρ is dominated by non-relativistic matter, this modified Friedmann equation can be rewritten as

$$\frac{H}{H_0} = \sqrt{\Omega_m a^{-3} + \Omega_\Lambda + \Omega_{r_c}} + \epsilon \sqrt{\Omega_{r_c}}, \quad (12)$$

where $\Omega_\Lambda = \kappa_4^2 \sigma / 3H_0^2$ is the effective cosmological constant for the brane tension and

$$\sqrt{\Omega_{r_c}} \equiv \frac{1}{2H_0 r_c} = \frac{\epsilon}{2} (1 - \Omega_m - \Omega_\Lambda), \quad (13)$$

defines the crossover scale in terms of the other cosmological parameters.

C. Perturbation Equations

The perturbed GN line element is written as:

$$ds^2 = -n^2(1 + 2\lambda A) dt^2 + 2n\lambda A_y dt dy + b^2(1 + 2\lambda \mathcal{R}) dx^2 + (1 + 2\lambda A_{yy}) dy^2, \quad (14)$$

in the longitudinal gauge where $\lambda \ll 1$ is an order parameter for bookkeeping purposes. These metric perturbations are governed by the master variable Ω [13] through the relations [14]

$$A = -\frac{1}{6b} \left(2 \frac{\partial^2 \Omega}{\partial y^2} + \frac{1}{n^2} \frac{\partial^2 \Omega}{\partial t^2} - \frac{1}{n^3} \frac{\partial n}{\partial t} \frac{\partial \Omega}{\partial t} - \frac{1}{n} \frac{\partial n}{\partial y} \frac{\partial \Omega}{\partial y} \right), \quad (15a)$$

$$A_y = +\frac{1}{bn} \left(\frac{\partial^2 \Omega}{\partial t \partial y} - \frac{1}{n} \frac{\partial n}{\partial y} \frac{\partial \Omega}{\partial t} \right), \quad (15b)$$

$$A_{yy} = +\frac{1}{6b} \left(\frac{\partial^2 \Omega}{\partial y^2} + \frac{2}{n^2} \frac{\partial^2 \Omega}{\partial t^2} - \frac{2}{n^3} \frac{\partial n}{\partial t} \frac{\partial \Omega}{\partial t} - \frac{2}{n} \frac{\partial n}{\partial y} \frac{\partial \Omega}{\partial y} \right), \quad (15c)$$

$$\mathcal{R} = +\frac{1}{6b} \left(\frac{\partial^2 \Omega}{\partial y^2} - \frac{1}{n^2} \frac{\partial^2 \Omega}{\partial t^2} + \frac{1}{n^3} \frac{\partial n}{\partial t} \frac{\partial \Omega}{\partial t} + \frac{1}{n} \frac{\partial n}{\partial y} \frac{\partial \Omega}{\partial y} \right). \quad (15d)$$

The master variable satisfies the wave, or master, equation

$$-\frac{\partial}{\partial t} \left(\frac{1}{nb^3} \frac{\partial \Omega}{\partial t} \right) + \frac{\partial}{\partial y} \left(\frac{n}{b^3} \frac{\partial \Omega}{\partial y} \right) - \frac{n}{b^5} k^2 \Omega = 0, \quad (16a)$$

$$-\frac{\partial^2 \Omega}{\partial u \partial v} + \frac{3}{2v} \frac{\partial \Omega}{\partial v} - \frac{k^2 r_c^2}{4v^2} \Omega = 0, \quad (16b)$$

in GN and null coordinates, respectively.

The master variable also satisfies the boundary condition

$$(\partial_y \Omega)_b = -\frac{\epsilon \gamma_1}{2H} \ddot{\Omega}_b + \frac{9\epsilon \gamma_3}{4} \dot{\Omega}_b - \frac{3(\epsilon \gamma_3 k^2 + \gamma_4 H^2 a^2)}{4H a^2} \Omega_b + \frac{3\epsilon r_c \kappa_4^2 \rho a^3 \gamma_4}{2k^2} \Delta. \quad (17)$$

The boundary value of the master variable Ω_b acts as a source to the brane metric perturbations $\Psi = A(y=0)$ and $\Phi = \mathcal{R}(y=0)$:

$$\Phi = +\frac{\kappa_4^2 \rho a^2 \gamma_1}{2k^2} \Delta + \frac{\epsilon \gamma_1}{4a r_c} \dot{\Omega}_b - \frac{\epsilon(k^2 + 3H^2 a^2) \gamma_1}{12H r_c a^3} \Omega_b, \quad (18a)$$

$$\Psi = -\frac{\kappa_4^2 \rho a^2 \gamma_2}{2k^2} \Delta + \frac{\epsilon \gamma_1}{4H r_c a} \ddot{\Omega}_b - \frac{3\epsilon H \gamma_4}{4a} \dot{\Omega}_b + \frac{\epsilon(k^2 r_c \gamma_4 + H a^2 \gamma_2)}{4r_c a^3} \Omega_b, \quad (18b)$$

where the dimensionless γ -factors

$$\gamma_1 = \frac{2\epsilon H r_c}{2\epsilon H r_c - 1}, \quad (19a)$$

$$\gamma_2 = \frac{2\epsilon r_c (\dot{H} - H^2 + 2\epsilon H^3 r_c)}{H(2\epsilon H r_c - 1)^2}, \quad (19b)$$

$$\gamma_3 = \frac{4\epsilon r_c (2\epsilon r_c \dot{H} - 3H + 6\epsilon H^2 r_c)}{9(2\epsilon H r_c - 1)^2}, \quad (19c)$$

$$\gamma_4 = \frac{4\epsilon(\epsilon r_c \dot{H} - H + 2\epsilon H^2 r_c)}{3H(2\epsilon H r_c - 1)^2}. \quad (19d)$$

With these relations, energy-momentum conservation of the matter on the brane simplify to yield

$$\ddot{\Delta} + 2H \dot{\Delta} - \frac{1}{2} \kappa_4^2 \rho \gamma_2 \Delta = -\frac{\epsilon \gamma_4 k^4}{4a^5} \Omega_b. \quad (20)$$

Eq. (16), (17) and (20) represent the complete equations of motion for the perturbations.

D. Initial Conditions

In order to fully specify the dynamics of perturbations, the equations of motion must be augmented by initial conditions, not only on the brane but also in the bulk. On the brane, the suppression of DGP modifications at $H r_c \gg 1$ means that initial conditions can be set as usual with adiabatic conditions. In the bulk, it is physically

sensible that all bulk perturbations are causally generated by perturbations on the brane; i.e., there should be no sources for Ω except the brane itself. This is equivalent to demanding that the bulk master variable vanish on the past Cauchy horizon:

$$\Omega(\mathcal{H}_-) = 0. \quad (21)$$

While the principal motivation for this assumption is causality, it is interesting to note that in the normal branch this is a necessary condition to avoid a curvature singularity in the bulk. To see this we substitute Eqs. (15) and (16a) into (14), and then calculate the full Riemann tensor in the normal branch. We find that the Riemann tensor tends to diverge on the past Cauchy horizon \mathcal{H}_- (where $b = 0$ and $v = 0$) in the normal branch unless Ω is correspondingly suppressed; for example,

$$R_{tyty} = -\frac{\lambda}{3} \frac{k^4 n^2 \Omega}{b^5} + \mathcal{O}(\lambda^2). \quad (22)$$

We shall see that this issue is related to an irregular singular point at the horizon at finite k in the master equation and requires that Ω be exponentially suppressed near \mathcal{H}_- , which is actually a stronger condition than Eq. (21).

E. Brane Gradient and Metric

The dynamical equations (17) and (20) are closed on the brane if the relationship between $(\partial_y \Omega)_b$ and Ω_b is known. From the perspective of the observer on the brane, the wave equation (16) for the master variable in the bulk simply serves to specify the dimensionless gradient

$$R \equiv \left(\frac{\partial_y \Omega}{\epsilon H \Omega} \right)_b. \quad (23)$$

We shall see that scaling and Green's function arguments can be used to extract this gradient in various limits.

Ultimately, we are most interested not in the brane gradient R , but the metric perturbations themselves. In particular the ratio of metric perturbations

$$g(a, k) \equiv \frac{\Phi + \Psi}{\Phi - \Psi} \quad (24)$$

plays a central role in modified gravity models as it vanishes in General Relativity if there is no anisotropic stress. Moreover in the parameterized post-Friedmann (PPF) formalism [15], it efficiently specifies metric perturbations for all scales. For the large scale regime $(k/Ha) \ll 1$, in General Relativity it is well known that the curvature perturbation on comoving slices ζ is conserved. This conservation law is a consequence of energy-momentum conservation and applies to DGP as well [3]. For the DGP model, we can express ζ in terms of Ω_b and Δ :

$$\zeta = \Phi + \frac{Ha}{\rho} \delta q = -\frac{\dot{H}a^2}{k^2} \Delta + \frac{Ha^2}{k^2} \dot{\Delta} - \frac{\epsilon \gamma_1 k^2}{12 H r_c a^3} \Omega_b. \quad (25)$$

The derivative of ζ can then be shown to be

$$\zeta' = -\frac{\epsilon}{12} \left(\frac{k}{Ha} \right)^2 \left(\frac{H r_c}{a} \right) \left[\frac{\gamma_1 \Omega_b' + (\gamma_1 - 9\gamma_3) \Omega_b}{r_c^2} \right], \quad (26)$$

where a prime indicates differentiation with respect to $\ln a$. One can also confirm that the following identity holds in DGP:

$$\Phi'' - \Psi' - \frac{H''}{H'} \Phi' - \left(\frac{H'}{H} - \frac{H''}{H'} \right) \Psi = -\frac{\epsilon \gamma_1}{12} \left(\frac{k}{Ha} \right)^2 \left(\frac{H r_c}{a} \right) \left[\frac{\Omega_b'' - \Omega_b' + 2H'H^{-2}(\gamma_1 H' + 2H)\Omega_b}{r_c^2} \right]. \quad (27)$$

Hence, we recover that

$$\zeta' \approx 0 \approx \Phi'' - \Psi' - \frac{H''}{H'} \Phi' - \left(\frac{H'}{H} - \frac{H''}{H'} \right) \Psi, \quad (28)$$

in the $k \rightarrow 0$ limit [3]. Given g , $\Phi = \Psi(g+1)/(g-1)$ and this ODE can be readily integrated to find Φ or Ψ given g and H .

Conversely at subhorizon scales $k/Ha \gg 1$, one can employ a “quasistatic ansatz” which assumes that gradients with respect to \mathbf{x} and y are of the same order and dominate over time derivatives (see §IV A for more details on this regime). This implies that the influence of the bulk through the brane gradient R is negligible, as it involves only one spatial derivative, and [16]

$$k^4 \Omega_b \approx 2Hr_c \frac{\gamma_4}{\gamma_3} \kappa_4^2 \rho a^5 \Delta. \quad (29)$$

Eq. (18) can be expressed as the Poisson equation [17]

$$\frac{\Phi - \Psi}{2} \approx \frac{\kappa_4^2 \rho a^2}{2k^2} \Delta, \quad (30)$$

for the quantity $(\Phi - \Psi)/2$ which enters into observables such as gravitational redshift and lensing. The quantity Ψ , which enters into the motion of non-relativistic matter is then specified by the relation

$$g \approx g_{\text{QS}} = -\frac{1}{3[1 - 2Hr_c \epsilon(1 + \dot{H}/3H^2)]}. \quad (31)$$

In both limits the dynamics of the perturbations are completely specified once $g(a, k)$ is known. Since $g(a, k)$ is determined in the quasistatic limit by the structure of the equations themselves, we concentrate on understanding the superhorizon regime in §III and §IV. We then seek a suitable interpolation between the two regimes in §V. This can then be used in the PPF formalism with publicly available codes [18] to generate the metric perturbations Φ and Ψ in an efficient manner.

III. METHODOLOGY

In this section we review two techniques, characteristic integration and the scaling ansatz, that have been used in the literature to solve numerically for DGP perturbations on large scales where bulk effects are important. In the following sections, we will use the scaling ansatz to develop the analytic approximations and the characteristic integration algorithm to test them.

A. Characteristic Integration

In order to model the behavior of perturbations in the DGP model, the characteristic integration (CI) algorithm [6, 19] constructs a direct finite difference solution to the bulk (16) and brane (20) equations of motion subject to the boundary condition (17). The code makes use of the null coordinates (u, v) , which implies that the brane is a *moving* boundary.

The natural computational domains of the CI algorithm for both branches are indicated in Figure 1. Initial data for the bulk field Ω must be supplied on the past null boundary of the domain. In addition, one must also specify the value of Δ , $\dot{\Delta}$ and $\dot{\Omega}_b$ at the intersection of the initial data surface and the brane. Because of the fact that this algorithm is based on null curves in the bulk, the initial condition (21) is very easy to approximate, we merely need to set $\Omega = 0$ on the initial null surface in the computational domain. As the initial scale factor of the simulation a_{init} is pushed further into the past, the output of the CI code will approach the desired solution with $\Omega(\mathcal{H}_-) = 0$, though in practice one finds that simulation results are stable to changes in a_{init} provided that it is below some threshold value (typically 10^{-3} for the simulations presented in the paper).

B. Scaling Ansatz

During epochs when the expansion rate on the brane is dominated by a single component, we expect the master variable on the brane to reach a scaling solution $\Omega_b \propto a^p$ for modes that are outside the horizon ($k/Ha \ll 1$). The boundary equation (17) then implies that the gradient term of Eq. (23) obeys

$$R = -\frac{1}{2}\gamma_1 \left(p^2 + \frac{\dot{H}}{H^2} p \right) + \frac{9}{4}\gamma_3 p - \frac{3\epsilon}{4}\gamma_4 + \frac{3}{2}Hr_c \frac{\kappa_4 \rho}{H^2} \gamma_4 a^3 \frac{\Delta}{k^2 \Omega_b}, \quad (32)$$

which gives the relationship between Ω_b and Δ and closes the dynamics on the brane.

To determine the gradient parameter R we make a similar scaling ansatz for the dependence of Ω on the GN coordinates in the bulk [3]

$$\Omega(t, y) = a^p(t)G(\epsilon H(t)y). \quad (33)$$

This ansatz is motivated by the distance in the bulk connected by a null worldline $dy = ndt$, i.e. a ‘‘horizon’’ in the bulk. For the self-accelerating branch

$$y_{\text{hor}} = aH \int_0^a \frac{d\tilde{a}}{\tilde{a}^2 H^2}, \quad (\epsilon = +1), \quad (34)$$

and Eq. (9) shows that $y = y_{\text{hor}}$ corresponds to the null line $u = 0$. With a power-law behavior for $H^2 \propto a^{-3(1+w)/2}$, $Hy_{\text{hor}} = 1/(2 + 3w)$ if $w > -2/3$.

For the normal branch, independently of the evolution of H

$$y_{\text{hor}} = \frac{1}{H}, \quad (\epsilon = -1), \quad (35)$$

which corrects Eq. (21) in Ref. [8]. Eq. (9) shows that $y = y_{\text{hor}}$ corresponds to the null line $v = 0$ on the normal branch and hence coincides with the coordinate singularity (see discussion below Eq. (10)).

The final condition introduced in Ref. [3] is that the initial data $G(\epsilon Hy_{\text{hor}}) = 0$ based on the assumption that bulk perturbations are generated causally from brane perturbations. This is entirely equivalent to Eq. (21) and compatible with the CI initial data as discussed above. Recall that $G(\epsilon Hy_{\text{hor}}) = 0$ is also required to keep the Riemann curvature finite in the normal branch.

The scaling technique can be extended to apply between different scaling regimes by iteratively solving for a time dependent $p(a)$ with the so-called dynamical scaling (DS) method [3]. However the CI method supersedes the DS method in accuracy and so we will not consider the latter further here. We instead use scaling arguments to develop analytic solutions in the next section.

IV. ANALYTIC SOLUTIONS

In this section we employ analytic techniques to obtain solutions for the metric perturbations modes that are either far inside or outside the horizon on the brane. We begin in §IV A by deriving the behavior of perturbations in the quasistatic regime $k/Ha \gg 1$, then we examine the opposite large scale limit $k/Ha \ll 1$ for cases where the expansion rate on the brane evolves as a simple power of the scale factor in §IV B, and finally in §IV C-IV D we turn to the behavior of superhorizon modes during de Sitter expansion.

A. Quasistatic Modes

In this subsection, we examine the behavior of modes when $k/Ha \gg 1$ in the context of the quasistatic approximation and derive the first order correction to g in Ha/k . (First order corrections to the quasistatic limit of DGP have also been considered by Amin et al. [20].)

If we make the assumption in the master wave equation (16a) that time derivatives of Ω can be neglected, we find that [16]

$$\Omega \approx c_1(1 + \epsilon Hy)^{k/Ha} + c_2(1 + \epsilon Hy)^{-k/Ha} \quad (36)$$

in the limit of $k/Ha \gg 1$. To ensure regularity of the master variable on the Cauchy horizon we need to set $c_1 = 0$ for the self-accelerating branch and $c_2 = 0$ for the normal branch. Therefore, the brane gradient becomes

$$R = -\frac{\epsilon k}{Ha} \left[1 + \mathcal{O}\left(\frac{Ha}{k}\right) \right]. \quad (37)$$

This analysis justifies the quasistatic assumption in §II E that the impact of R on the brane is negligible compared with $(k/Ha)^2$ terms in the brane boundary equation (17).

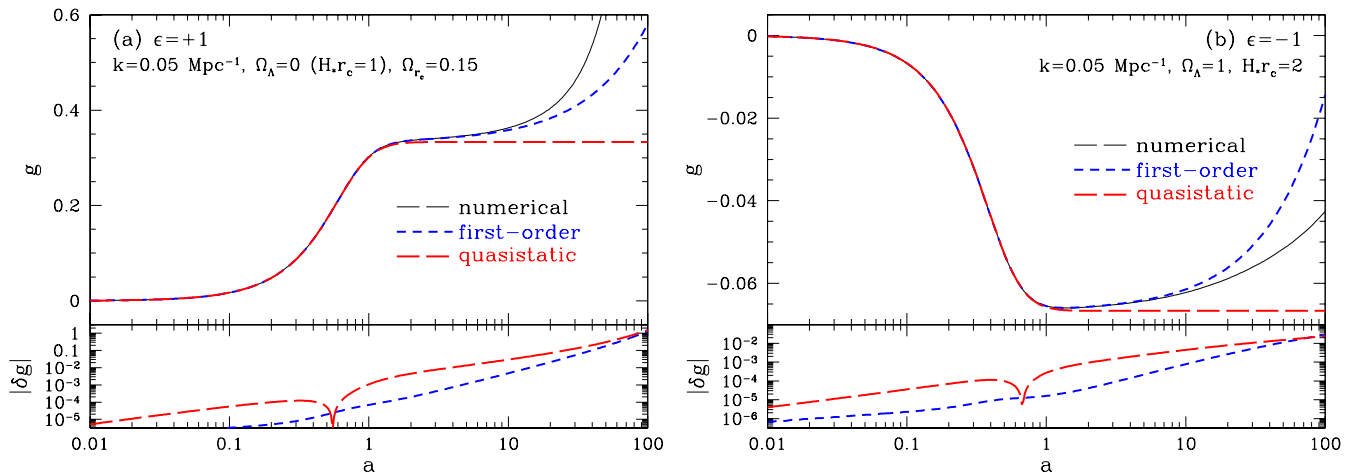


FIG. 2: Comparison of simulation results (black solid) to the quasistatic approximation at zeroth order (red long-dashed) and with first order Ha/k corrections (blue short-dashed). In both the self-accelerating and normal branches, the residuals δg between the approximation and simulation results are roughly an order of magnitude smaller when first order corrections are included for $a \leq 1$. The first order correction becomes invalid as $k/Ha \rightarrow 0$ as the mode exits the horizon during the de Sitter epoch $a \gg 1$. Also note that we recover the general relativity result $g = 0$ in the early time limit $Hr_c \rightarrow \infty$ or, equivalently, $a \rightarrow 0$.

Putting this into the expressions for the metric potentials (18) and expanding in inverse powers of k/Ha we obtain:

$$\Phi + \Psi = \frac{\kappa_4^2 \rho a^2 \Delta}{k^2} \left[\frac{\epsilon \gamma_1^2}{9Hr_c \gamma_3} + \frac{\gamma_4(4Hr_c \gamma_4 - 3\gamma_3)}{3\gamma_3^2} \frac{Ha}{k} + \mathcal{O}\left(\frac{H^2 a^2}{k^2}\right) \right], \quad (38a)$$

$$\Phi - \Psi = \frac{\kappa_4^2 \rho a^2 \Delta}{k^2} \left[1 - \frac{\gamma_4}{3\gamma_3} \frac{Ha}{k} + \mathcal{O}\left(\frac{H^2 a^2}{k^2}\right) \right], \quad (38b)$$

which in turn yields the first order correction to g from the brane gradient

$$g = g_{QS} + \frac{\epsilon \gamma_4 [\gamma_1^2 + 3\epsilon Hr_c (4Hr_c \gamma_4 - 3\gamma_3)]}{9Hr_c \gamma_3^2} \frac{Ha}{k} + \mathcal{O}\left(\frac{H^2 a^2}{k^2}\right). \quad (39)$$

In Fig. 2, we show a comparison between simulation results and this formula when only the leading order term is retained (i.e. the standard quasistatic approximation) and when the next to leading order term is retained (i.e. a “first-order” quasistatic approximation).

The first order result gives a more accurate approximation to the simulations results in the $k/Ha \gg 1$ regime. It extends either the accuracy or the regime of validity in k/Ha of the quasistatic approximation by about an order of magnitude. In the example in Fig. 2, it corrects the quasistatic approximation at the 10^{-3} level for $a \leq 1$.

For $a \gg 1$, even modes that are far within the current horizon eventually exit the horizon. Note that the first order correction is unbounded as $k/Ha \rightarrow 0$. The numerical solutions on the self accelerating branch are also unbounded but the first order correction does not capture this behavior accurately. On the normal branch, the numerical solutions remain finite and again the behavior is not captured by the approximation. This problem applies equally to near horizon modes at $a \sim 1$. We therefore now turn to study the large scale behavior of g .

B. Power-law Expansion

In the superhorizon regime $k/Ha \ll 1$, there is no universally-valid closed-form solution for g . In this subsection, we thus restrict ourselves to the situation where the expansion of the brane is well described by a simple power law in the scale factor a . We can then take

$$H^2 \propto a^{-3(1+w)}, \quad \dot{H} \approx -\frac{3}{2}(1+w)H^2. \quad (40)$$

Here, the constant w is an effective equation of state parameter not to be confused with the equation of state of the matter on the brane. The scaling ansatz (33) reduces the master wave equation (16) down to an ODE for the scaling function G of the form [see [3] Eq. (43)]

$$\frac{d^2 G}{dx^2} + \mathcal{P}(x) \frac{dG}{dx} + \mathcal{Q}(x)G = 0, \quad (41)$$

where $x = \epsilon Hy$. The past Cauchy horizon in the bulk \mathcal{H}_- corresponds to

$$x_{\text{hor}} = \epsilon Hy_{\text{hor}} = \begin{cases} 1/(2+3w), & \epsilon = +1, w > -2/3 \\ \text{undefined}, & \epsilon = +1, w \leq -2/3 \\ -1, & \epsilon = -1, \end{cases} \quad (42)$$

while the brane is always at $x = 0$. The fact that the horizon position is undefined in the self-accelerating case when $w < -2/3$ is a consequence of the behavior of the Gaussian normal coordinates in the bulk. This is illustrated in Fig. 3, where we see that if the effective equation of state $w < -2/3$ at early times, $t = \text{constant}$ hypersurfaces fail to intersect \mathcal{H}_- when $\epsilon = +1$. (This also happens in the normal branch when $w = -1$, but this pathology manifests itself differently below.) We now seek solutions to Eq. (41) in the superhorizon $k/Ha \rightarrow 0$ limit for $x \in (0, x_{\text{hor}})$ on the self-accelerating branch (when x_{hor} is finite) and for $x \in (x_{\text{hor}}, 0) = (-1, 0)$ on the normal branch.

A straightforward analysis of the poles of \mathcal{P} and \mathcal{Q} reveals that $x = 1/(2+3w)$ and $x = 2/(3w+1)$ are regular singular points of the ODE (41). The first of these is coincident with the bulk horizon when $\epsilon = +1$ and $w > -2/3$. The second singularity occurs outside the range $x \in [-1, 1/(2+3w)]$ for all w , and hence is not relevant to our problem.

In addition to the regular singular points, there is an irregular singular point at $x = -1$; i.e., coincident with the bulk horizon when $\epsilon = -1$. The nature of this singularity is apparent if we expand \mathcal{Q} in a Laurent series about $x = -1$:

$$\mathcal{Q}(x) = -\frac{3}{4} \frac{k^2}{H^2 a^2} \frac{1+w}{(1+x)^3} + \dots \quad (43)$$

We see that this third order pole disappears if either $w = -1$ or $k/Ha = 0$.

We use the technique of matched asymptotic expansion to obtain the solution in the $k/Ha \ll 1$ limit. Away from the pole at $x = -1$, we can set $k = 0$ in Eq. (41) to obtain the outer (or near-brane) solution valid for $w \neq -2/3$

$$G(x) = c_1(1+x)^p + c_2(1+x)^{3/2} [1 - (2+3w)x]^{(2p-3)/(4+6w)}. \quad (44)$$

Here, c_1 and c_2 are arbitrary constants.

The outer solution is sufficient for the consideration of the self accelerating branch where $x \in (0, x_{\text{hor}})$. When $w > -2/3$, the condition that $\Omega(\mathcal{H}_-) = 0$ is equivalent to setting $G(1/(2+3w)) = 0$, which implies that $c_1 = 0$ when $p > 3/2$. Under these conditions, the brane gradient is

$$R = \left(\frac{1}{G} \frac{dG}{dx} \right)_{x=0} = 3 - p. \quad (45)$$

For $p < 3/2$, strictly speaking no solution exists for constant w . However in the real universe, one would expect deviations from other components that break the $w = \text{const.}$ assumption to make the c_2 solution finite at the horizon and c_1 dominant at the brane. Hence we can assign $R = p$ to the $p < 3/2$ modes.

For $w < -2/3$ as in the case of the de Sitter regime considered below, x_{hor} in principle diverges. In practice x_{hor} always remains finite at finite time given the preceding epochs of radiation and matter domination but increases without bound.

Turning our attention to the normal branch, we require an inner (or near-horizon) solution close to the irregular singular point at $x = -1$. The Laurent expansion (43) implies that we cannot set $k = 0$ *a priori*; i.e., the k/Ha contributions to the ODE are not subdominant near $x = -1$. To overcome this, we transform to the variable

$$\xi = \frac{Ha}{k} \sqrt{\frac{1+x}{3(1+w)}}. \quad (46)$$

In terms of this new coordinate, the horizon is at $\xi = 0$ and the brane is at $\xi \gg 1$. The inner solution is specified by setting $k = 0$ in the transformed equation for ξ and takes the form

$$G(x(\xi)) = \xi^{p+3/2} \left[c_3 I_{3/2-p} \left(\frac{1}{\xi} \right) + c_4 K_{p-3/2} \left(\frac{1}{\xi} \right) \right], \quad (47)$$

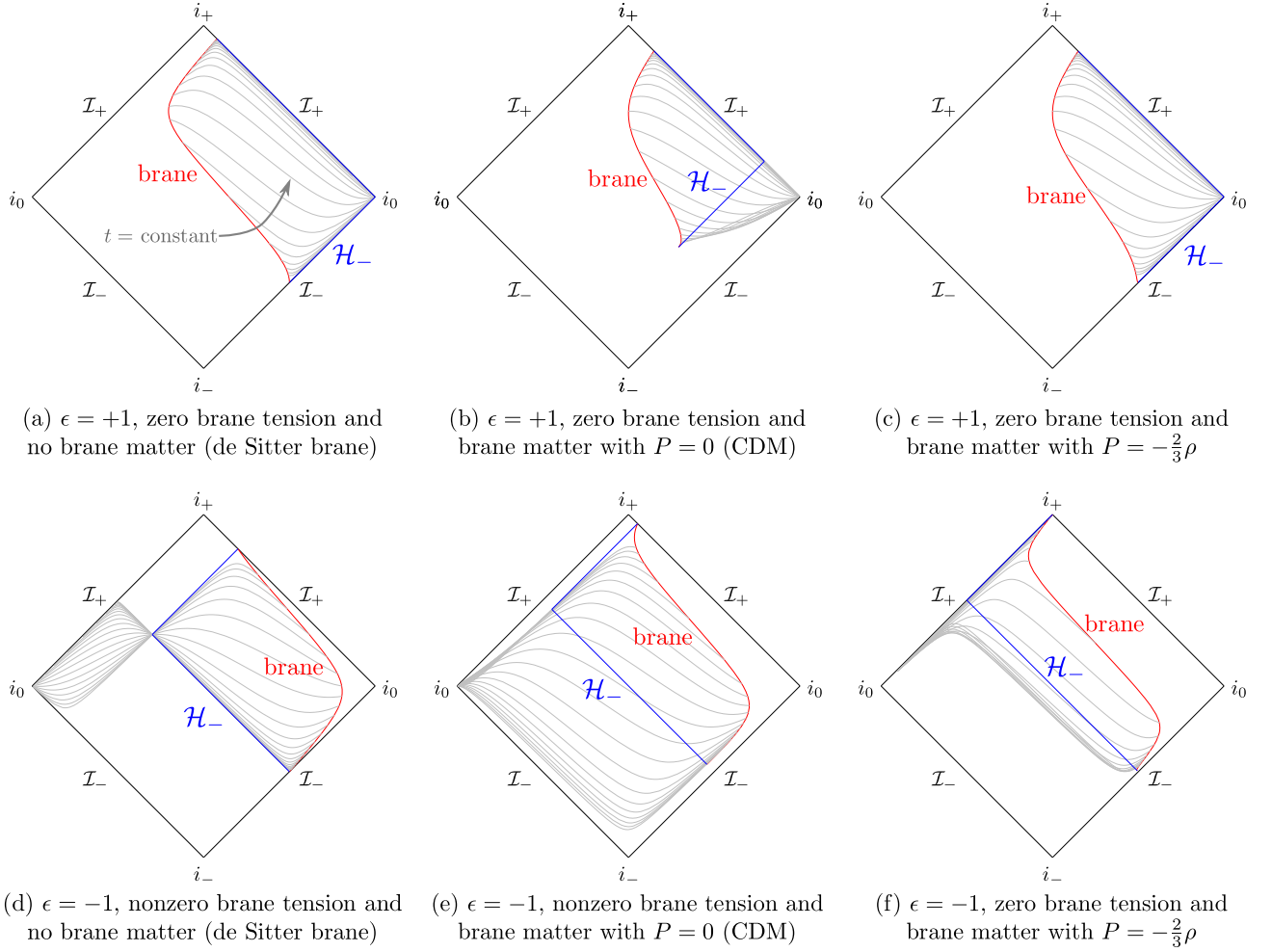


FIG. 3: Conformal diagrams showing the behavior of the $t = \text{constant}$ hypersurfaces in the space spanned by the (u, v) coordinates (ρ and P are the density and pressure of brane matter, respectively). The scaling ansatz is expected to be informative when these surfaces intersect the brane's past Cauchy horizon \mathcal{H}_- . This is indeed the case in the self-accelerating and normal branches when the brane transitions from early matter domination to a late time de Sitter phase, as in panels (b) and (e) respectively. However, when the brane undergoes purely de Sitter like expansion, as in (a) and (d), the $t = \text{constant}$ curves fail to pierce \mathcal{H}_- . In these scenarios, it is impossible to impose the initial condition $\Omega(\mathcal{H}_-) = 0$ in the context of the scaling ansatz. Finally, there are some choices of brane matter and tension where the behavior of the $t = \text{constant}$ surfaces are qualitatively different on the two branches. An example of this is in panels (c) and (f), where the brane matter has $P = -\frac{2}{3}\rho$. In the normal branch $t = \text{constant}$ surfaces cover \mathcal{H}_- and we expect the scaling calculation to be applicable, while the opposite is true for the self-accelerating case.

where I and K are modified Bessel functions of the first and second kind, respectively.

On the normal branch, the boundary condition that $\Omega(\mathcal{H}_-) = 0$ implies $G = 0$ at $\xi = 0$. Taking note of the asymptotic expansions of the Bessel functions for $\xi \ll 1$,

$$I_{3/2-p} \left(\frac{1}{\xi} \right) \sim \exp \left(\frac{1}{\xi} \right), \quad K_{p-3/2} \left(\frac{1}{\xi} \right) \sim \exp \left(-\frac{1}{\xi} \right), \quad (48)$$

we see that we must set $c_3 = 0$ in the near-horizon G solution (47).

Finally we match the c_4 inner solution (47) to the outer solutions (44) at $\xi \gg 1$ but $(1+x) \ll 1$ to obtain the global approximate solution

$$G(x(\xi)) \propto \begin{cases} \xi^{p+3/2} K_{p-3/2}(1/\xi), & p \geq 3/2, \\ \xi^{p+3/2} K_{p-3/2}(1/\xi) [1 - (2+3w)x]^{(2p-3)/(4+6w)}, & p < 3/2. \end{cases} \quad (49)$$

Substituting this global solution into the exact equation (41) for G , we see that the residuals are $\mathcal{O}(k/Ha)$ and

converge uniformly in the interval $0 < 1 + x < 1$; moreover numerical integration of Eq. (41) confirms these solutions. Given $\xi^2 \propto (1 + x)$, this solution implies that $p \geq 3/2$ matches onto the c_1 mode $p < 3/2$ the c_2 mode of Eq. (44) for the normal branch. Before moving on, we note that these expressions for G in the normal branch only hold when the irregular singular point at $x = -1$ is present; i.e. when $w > -1$ and k is finite. In other words, the scaling approximation will not be informative in the purely de Sitter case $w = -1$, as could have been surmised from panel (d) in Fig. 3.

To summarize, we have shown that under the scaling ansatz $\Omega(t, y) = a^p G(\epsilon H y)$ combined with the initial data $G(\epsilon H y_{\text{hor}}) = 0$ the brane gradient satisfies

$$R = \begin{cases} 3 - p, & \epsilon = +1, w > -2/3, p \geq 3/2, \\ p, & \epsilon = +1, w > -2/3, p < 3/2, \\ p, & \epsilon = -1, w \neq -1, p \geq 3/2, \\ 3 - p, & \epsilon = -1, w \neq -1, p < 3/2 \end{cases} \quad (50)$$

in the $k/Ha \rightarrow 0$ limit.

The preferred values for p are determined by the brane boundary equation through the density source. For example in the matter dominated phase when $w = 0$, the matter density fluctuation $\Delta \propto a$ acts as an external source to Ω_b in the boundary equation (17) so that for $k/Ha \ll 1$, the particular mode is $p = 4$. For the self accelerating branch the matter dominated solution is therefore $R = -1$ and

$$g_{\text{SH}} = \frac{9}{8Hr_c - 1}, \quad \epsilon = +1, \quad (51)$$

whereas on the normal branch $R = 4$ and

$$g_{\text{SH}} = -\frac{1}{2Hr_c + 1}, \quad \epsilon = -1. \quad (52)$$

These relations close the perturbation equations on the brane.

C. De Sitter Scaling

The late time de Sitter phase carries an effective equation of state of $w = -1$ and is a special case for the scaling solutions both on the self-accelerating and normal branch. The horizon on the self-accelerating branch goes to infinity while the horizon on the normal branch is no longer an irregular singular point of the master equation (16a).

Given the matter in the universe, a pure de Sitter expansion is never fully reached and it is important to consider the manner in which the de Sitter phase is approached. The Hubble parameter approaches a constant

$$\frac{H_\star}{H_0} = \sqrt{\Omega_\Lambda + \Omega_{r_c}} + \epsilon \sqrt{\Omega_{r_c}} \quad (53)$$

for a scale factor $a \gg a_\star$ where $H(a_\star) \equiv \sqrt{2}H_\star$ and

$$\Omega_m a_\star^{-3} = \Omega_\Lambda + (4 - 2\sqrt{2})\Omega_{r_c} (1 + \epsilon \sqrt{1 + \Omega_\Lambda/\Omega_{r_c}}). \quad (54)$$

Note that if $\Omega_\Lambda/\Omega_{r_c} \gg 1$, $a_\star = (\Omega_m/\Omega_\Lambda)^{1/3}$ as usual. If $\Omega_\Lambda/\Omega_{r_c} \ll 1$

$$a_\star = \begin{cases} \left[\frac{\Omega_m}{4(2 - \sqrt{2})\Omega_{r_c}} \right]^{1/3}, & \epsilon = +1, \\ \left[\frac{\Omega_m}{(\sqrt{2} - 1)\Omega_\Lambda} \right]^{1/3}, & \epsilon = -1. \end{cases} \quad (55)$$

In both cases Hr_c also approaches a constant

$$H_\star r_c = \frac{1}{2} \left[\sqrt{1 + \frac{\Omega_\Lambda}{\Omega_{r_c}}} + \epsilon \right]. \quad (56)$$

We shall see that the residual effects from the preceding matter dominated phase determine the behavior of the perturbations on the brane. Likewise in Fig. 3, we see that the pathologies in panels (a) and (d) disappear with the addition of matter in (b) and (e).

1. Bulk solutions

If we take a pure de Sitter limit where $\dot{H} = 0$, the master equation (16a) becomes

$$(1+x)^2 \frac{\partial^2 \Omega}{\partial x^2} - 2(1+x) \frac{\partial \Omega}{\partial x} - \Omega'' + 3\Omega' - \frac{k^2}{a^2 H^2} \Omega = 0, \quad (57)$$

where recall $' = d/d \ln a$.

The general solution to the pure de Sitter master equation for $k/Ha \ll 1$ is

$$\Omega = a^p [c_1(1+x)^p + c_2(1+x)^{3-p}]. \quad (58)$$

This solution in fact corresponds to the $w = -1$ limit of the general constant w scaling solution (44) but in this case separability in a and x is guaranteed, not an ansatz.

One might therefore expect the scaling results to hold: $c_1 = 0$ ($R = 3-p$) for the self-accelerating branch and $c_2 = 0$ ($R = p$) for the normal branch for the fastest growing modes. However, direct application of the condition $G(x_{\text{hor}}) = 0$ fails to be informative in both cases due to a change in the nature of the x_{hor} point. For the self-accelerating branch, its value diverges and for the normal branch it is no longer an irregular singular point of the master equation. This can also be seen in Fig. 3, where we see that if the brane undergoes a purely de Sitter expansion, the $t = \text{constant}$ hypersurfaces do not intersect the past horizon and it is impossible to impose the initial condition $\Omega(\mathcal{H}_-) = 0$ in the scaling approximation.

To restore the information lost in the pure de Sitter limit, we must consider the preceding matter dominated expansion as in panels (b) and (e) of Fig. 3. For the self-accelerating branch, the matter dominated phase leads to a finite but growing $x_{\text{hor}} \sim aH_*^2/\Omega_m H_0^2$. The c_1 solution however does not depend on the evolution of $H(a)$ and so even given this preceding phase its contribution to Ω at the horizon increases as $(1+x_{\text{hor}})^p$ for $p > 0$. Hence the c_1 contribution must be negligible near $x \sim 0$ in order to satisfy the initial data $G(x_{\text{hor}}) = 0$. The form of the c_2 solution does depend on the evolution of $H(a)$ and hence it is plausible that the preceding matter dominated epoch induces a correction of the form $(1-x/x_{\text{hor}})$ as it does in the matter dominated limit [see Eq. (44)]. This correction has negligible impact near $x = 0$ and so we again obtain

$$R = 3 - p, \quad \epsilon = +1, \quad (59)$$

for the solution on the self-accelerating branch. We shall see that this line of reasoning is borne out by the more detailed Green's function calculation below.

On the normal branch, restoring a trace amount of matter has more dramatic effects. Defining

$$h_m \equiv \frac{H^2 - H_*^2}{H_*^2} \propto a^{-3}, \quad (60)$$

we obtain $H'/H \approx -(3/2)h_m$. In Eq. (8), the zero of n is shifted beyond the horizon $x < -1$ and the master equation (16a) regains an irregular singular point at finite k/Ha .

We can transform to the variable

$$\xi = \frac{Ha}{k} \sqrt{\frac{1+x}{3h_m}} \quad (61)$$

and again repeat the asymptotic matching of the interior $k = 0$ and exterior $k = 0$ solutions. As with constant w the interior solutions are given by Eq. (47). For $p > 3/2$ they again match onto the c_1 solution with $R = p$. For $p < 3/2$, it is important to consider an intermediate solution at finite h_m but $k = 0$. The interior solution matches onto the $(1+x)^{3/2}$ rather than the $(1+x)$ piece of this solution and in general can stimulate both the c_1 and the c_2 pieces of the exterior solution. From explicit solutions of these equations, we find that as $h_m \rightarrow 0$ the c_2 piece where $R = 3-p$ generally dominates given its larger growth with $(1+x)$. We shall see however that this leading order behavior is forbidden by the brane boundary equation.

2. Brane boundary

As in the matter dominated limit, certain values of the scaling index p are picked out by the boundary equation (32). Once the matter contribution to the expansion becomes negligible $\kappa_4^2 \rho/H^2 \ll 1$ and the matter conservation law

(20) requires that density perturbations obey $\Delta = \Delta_0 + \Delta_1(a/a_*)^{-2}$ where Δ_0 and Δ_1 are constants, i.e. to leading order, density fluctuations freeze out but with some stimulation of a decaying mode at the de Sitter transition.

While this behavior of Δ is the same as in General Relativity with dark energy, the particular mode here does not drive the leading order behavior of the metric perturbations Φ and Ψ . Note that the boundary equation (17) and master equation (16a) requires a constant response in Ω_b

$$\Omega_b = \frac{2\epsilon Hr_c \kappa_4^2 \rho a^3}{k^2 H^2} \Delta_0, \quad (62)$$

where the specific coefficient applies to $R = p = 0$. By virtue of Eq. (18), this mode carries no source to Φ and Ψ and as we shall see is the relevant particular mode for the normal branch [see Eq. (83)]. Hence their evolution is typically governed instead by the homogeneous Δ source free modes in Ω_b . If the source free modes decay faster than $p = -2$, then the next to leading order scaling of Δ_1 will dominate instead. On the self accelerating branch, we shall see that the fastest growing modes have $p > 0$ and again the leading order particular contribution does not dominate the metric evolution.

Now let us consider these homogeneous modes. We obtain from Eq. (32)

$$p(p-3) + \frac{1}{\epsilon Hr_c} + \frac{2\epsilon Hr_c - 1}{\epsilon Hr_c} R = 0. \quad (63)$$

For the self-accelerating branch, the condition $R = 3 - p$ ($c_1 = 0$) gives

$$p = 2, 3 - \frac{1}{Hr_c}, \quad \epsilon = +1, \quad (64)$$

where note that if $\Omega_\Lambda = 0$, $Hr_c \rightarrow 1$ and both solutions return $p = 2$. This analysis justifies the selection of the $p = 2$ mode in [3].

For the normal branch, taking $R = p$ ($c_2 = 0$) gives

$$p = 1, -\frac{1}{Hr_c}, \quad \epsilon = -1 \quad (65)$$

Here $p < 3/2$ and so in principle the $R = 3 - p$ mode should dominate leading to a contradiction. If we instead assume $R = 3 - p$, Eq. (63) requires that either $p = 2$ or $p = 3 + 1/Hr_c$; in either case, $p > 3/2$ and we again reach a contradiction. Therefore, no solution of this type can satisfy both $G(x_{\text{hor}}) = 0$ and the brane boundary condition.

Since the details of the matter to de Sitter transition are important for the $R = 3 - p$ mode whereas they are not for the $R = p$ mode, we conjecture that solutions with $p < 3/2$ should exist if corrections near the singularity prevent the c_2 mode in Eq. (58) from completely dominating.

If we further assume that there exist modes where $R = p$ is the dominant mode at $p < 3/2$ we obtain the modes in Eq. (65). In principle though, we can obtain a spectrum of modes with mixed $R = p$ and $R = 3 - p$ behavior. We shall see that the numerical CI solution implies that $p = 1$ is indeed the dominant mode for Ω . However, this mode has no effect on the brane metric parameters Φ and Ψ . Hence the important $k/Ha \rightarrow 0$ mode is $p = -1/Hr_c$, but that is a decaying mode in Ω . This opens up the possibility that k -dependent modes eventually dominate the evolution in the de Sitter epoch. To study this behavior and verify the conjectures involving the c_2 mode for both the self-accelerating and normal branch, we require a more complete Green's function analysis.

D. De Sitter Green's Function

To gain further insight into solutions in the de Sitter epoch, we can recast the perturbation equations as a canonical scattering problem via the transformation

$$\Omega(t, y) = (1 + \epsilon Hy)^{3/2} a^{3/2}(t) \varphi(t, y), \quad (66)$$

and define a new bulk variable z :

$$z = \frac{\ln(1 + \epsilon Hy)}{\epsilon H}, \quad y = \frac{e^{\epsilon Hz} - 1}{\epsilon H}. \quad (67)$$

The bulk manifold is defined by $z \in [0, \infty)$ for both branches. The new bulk variable satisfies a simple wave equation and boundary condition

$$\left(\frac{\partial^2}{\partial t^2} - \frac{\partial^2}{\partial z^2} + \frac{k^2}{a^2} \right) \varphi = 0, \quad (68a)$$

$$\left(\frac{\partial \varphi}{\partial z} \right)_{z=0} = -\frac{\epsilon r_c}{2Hr_c - \epsilon} \left(\frac{\partial^2 \varphi}{\partial z^2} \right)_{z=0} - \frac{\epsilon H(3Hr_c - 2\epsilon)}{4(2Hr_c - \epsilon)} \varphi_b + \frac{2\epsilon \kappa_4^2 r_c \rho a^{3/2}}{k^2(2Hr_c - \epsilon)} \Delta, \quad (68b)$$

where we have set $\varphi_b(t) = \varphi(t, 0)$ and made use of Eq. (68a) to remove time derivatives of φ . The equation of motion for Δ reduces to

$$\ddot{\Delta} + 2H\dot{\Delta} - \frac{\kappa_4^2 \rho H r_c}{2Hr_c - \epsilon} \Delta = \frac{\epsilon k^4}{3(2Hr_c - \epsilon) a^{7/2}} \varphi_b. \quad (69)$$

Examining equations (68), we see that Δ can be viewed as a brane-localized source for the bulk φ field. From linearity, it follows that the general solution for φ should be of the form

$$\varphi = \varphi^{(h)} + \varphi^{(p)}, \quad (70)$$

where $\varphi^{(h)}$ is the general homogeneous solution for Eq. (68) when $\Delta = 0$, and $\varphi^{(p)}$ is a particular solution when Δ is nonzero and determined from Eq. (69).

Let us now concentrate on the solution of the homogeneous system where $\varphi^{(h)}$ and its first time derivative $\dot{\varphi}^{(h)}$ are known at an initial time, say $t = 0$. Then, the value of $\varphi^{(h)}$ at some later time t and position z is given by

$$\begin{aligned} \varphi^{(h)}(t, z) = \int_0^\infty dz' \left[\varphi^{(h)}(t', z') \frac{\partial}{\partial t'} G_-(t, t'; z, z') - G_-(t, t'; z, z') \frac{\partial}{\partial t'} \varphi^{(h)}(t', z') \right]_{t'=0} + \\ \frac{\epsilon r_c}{2Hr_c - \epsilon} \left[\varphi^{(h)}(t', z') \frac{\partial}{\partial t'} G_-(t, t'; z, z') - G_-(t, t'; z, z') \frac{\partial}{\partial t'} \varphi^{(h)}(t', z') \right]_{t'=0, z'=0}, \quad (71) \end{aligned}$$

where G_- is the retarded Green's function. Though this formal solution of the initial value problem only involves G_- , we will also consider the advanced Green's function G_+ to facilitate comparison with the scaling solutions of §IV C. Both Green's functions satisfy

$$\left(\frac{\partial^2}{\partial t^2} - \frac{\partial^2}{\partial z^2} + \frac{k^2}{a^2} \right) G_\pm(t, t'; z, z') = -\delta(t - t') \delta(z - z'), \quad (72)$$

with boundary conditions

$$0 = \left\{ \left[\frac{\partial}{\partial z_{<}} + \frac{\epsilon r_c}{2Hr_c - \epsilon} \frac{\partial^2}{\partial z_{<}^2} + \frac{\epsilon H(3Hr_c - 2\epsilon)}{4(2Hr_c - \epsilon)} \right] G_\pm(t, t'; z, z') \right\}_{z_{<}=0}, \quad (73a)$$

$$0 \leq \Delta z \pm \Delta t \Rightarrow G_\pm(t, t'; z, z') = 0, \quad (73b)$$

where $z_{<} = \min(z, z')$, $z_{>} = \max(z, z')$, $\Delta t = t - t'$, and $\Delta z = |z - z'|$. The boundary condition (73b) ensures that the initial condition $\Omega(\mathcal{H}_-) = 0$ will be satisfied by Eq. (71) for $t > 0$. Note that \mathcal{H}_- corresponds to $t \rightarrow -\infty$ and $z \rightarrow \infty$, yet the boundary condition (73b) is imposed at finite values of the coordinates. This is in contrast to the scaling approach, where the condition $\Omega = 0$ is enforced on \mathcal{H}_- directly. Therefore, unlike the scaling solution, the Green's function approach is not compromised by the fact that Gaussian normal coordinates do not cover the past horizon for a de Sitter brane. That is, it is not necessary to impose conditions on the Green's function at \mathcal{H}_- to ensure that the solution (71) is consistent with $\Omega(\mathcal{H}_-) = 0$.

Using separation of variables and other standard techniques, the advanced and retarded Green's functions can be expressed as

$$G_\pm(t, t'; z, z') = \int_{-\infty}^{+\infty} d\nu \mathcal{G}_\pm(t, t'; z, z' | \nu), \quad (74a)$$

$$\mathcal{G}_\pm(t, t'; z, z' | \nu) = \frac{T_\nu(t) T_\nu^*(t') [f_\mp(\nu) e^{\pm i\nu H |z - z'|} + f_\pm(\nu) e^{\pm i\nu H (z + z')}] }{2i\nu H f_\mp(\nu)}, \quad (74b)$$

Green's function	resonant mode	frequency ν	temporal scaling p	brane gradient R
retarded G_-	A_1	$-i\epsilon/2$	$(3 + \epsilon)/2$	1
	A_2	$-i(3\epsilon/2 - \omega)$	$3(1 + \epsilon)/2 - \omega$	$\epsilon\omega$
	B_m ($m = 1, 2, \dots$)	im	$3/2 - m$	$\gamma_1(9 - 4\epsilon\omega - 4m^2)/8$
advanced G_+	C_1	$i\epsilon/2$	$(3 - \epsilon)/2$	1
	C_2	$i(3\epsilon/2 - \omega)$	$3(1 - \epsilon)/2 + \omega$	$\epsilon\omega$
	D_m ($m = 1, 2, \dots$)	im	$3/2 - m$	$\gamma_1(9 - 4\epsilon\omega - 4m^2)/8$

TABLE I: Resonances of the retarded and advanced Green's functions as determined by the poles of \mathcal{G}_- and \mathcal{G}_+ , respectively. ($\omega = 1/Hr_c$). Note that the $A_{1,2}$ and $C_{1,2}$ excitations give rise to late time resonant modes of the form $\Omega \propto a^p(1 + \epsilon Hy)^R$, while the B_m and D_m modes have more complicated y dependence.

The two terms represent propagation directly from z' to z or through reflection off of the boundary. The functions T_ν satisfy

$$\left(\frac{\partial^2}{\partial t^2} + \frac{k^2}{a^2} + H^2\nu^2\right)T_\nu(t) = 0, \quad \int_{-\infty}^{+\infty} d\nu T_\nu(t)T_\nu^*(t') = \delta(t - t'), \quad (75)$$

and f_\pm follow from the boundary condition (73a):

$$f_\pm(\nu) = (2\epsilon\nu \pm i)(3iHr_c - 2i\epsilon \pm 2\epsilon Hr_c\nu). \quad (76)$$

Explicitly, the temporal mode functions are given by

$$T_\nu(t) = \left(\frac{k}{2H}\right)^{i\nu} \left(\frac{H\nu}{\sinh \pi\nu}\right)^{1/2} J_{-i\nu}\left(\frac{k}{aH}\right). \quad (77)$$

Here, $J_{-i\nu}$ is the Bessel function of the first kind with order $-i\nu$.

Now, in order to evaluate the righthand side of Eq. (74a), we close the contour of integration in the upper-half of the complex ν plane when $\mp\Delta t > \Delta z$, and in the lower-half plane otherwise. This gives

$$G_\pm(t, t'; z, z') = \Theta(\mp\Delta t - \Delta z) \left[2\pi i \sum \text{Res } \mathcal{G}_\pm(t, t'; z, z'|\nu) - \int_{\Gamma_+} d\nu \mathcal{G}_\pm(t, t'; z, z'|\nu) \right]. \quad (78)$$

In this expression, the sum is over the residues of the poles of $\mathcal{G}_\pm(t, t'; z, z'|\nu)$ in the upper-half of the complex ν plane, and the contour Γ_+ represents the infinitely large semi-circle used to close the integration path. The poles of $\mathcal{G}_\pm(t, t'; z, z'|\nu)$ represent resonant excitations that will dominate the late time behavior of our system, and are listed in Table I. The A and C resonances listed in the table arise from zeros in $f_\pm(\nu)$ in Eq. (76), while the B and D modes are associated with divergences in the $T_\nu(t)$ functions. In what follows, we will neglect the Γ_+ integration and represent the Green's function as a sum over resonances.

It is instructive to relate the A and C resonances to the preferred modes in the scaling approach. The scaling solution of Eq. (58) corresponds to

$$\varphi(t, y) = c_1 e^{(p-3/2)H(t+\epsilon z)} + c_2 e^{(p-3/2)H(t-\epsilon z)}. \quad (79)$$

Each term represents a wave traveling towards or away from the brane depending on the choice of branch, and the boundary equation satisfied by φ can be interpreted as a reflection condition on these waves. Comparing the resonances from the poles of \mathcal{G}_\pm to Eq. (79), we see that the $A_{1,2}$ resonances of the *retarded* Green's function correspond to scaling solutions with $c_1 = 0$ in the self-accelerating branch and $c_2 = 0$ in the normal branch. Conversely, the $C_{1,2}$ *advanced* resonances have $c_2 = 0$ and $c_1 = 0$ for the self-accelerating and normal branches, respectively. The causality condition (21) picks out the retarded solution in each branch, which in turn implies that $c_1 = 0$ and $R = 3 - p$ for the self-accelerating branch, while $c_2 = 0$ and $R = p$ for the normal branch. This analysis verifies our conjectures of the previous section based on extending the de Sitter scaling solutions to include trace amounts of matter to specify the initial data.

In order to facilitate the comparison of simulation results with the predictions of the Green's function analysis, we hereafter restrict our attention to the retarded Green's function and assume that the field point (t, z) is on the brane and deep in the de Sitter era; i.e. $k/Ha(t) \ll 1$. The asymptotic form of G_- in this limit is

$$G_-(t, t'; 0, z') \approx -\frac{8i\epsilon Hr_c}{\gamma_1\pi} \int_{-\infty}^{+\infty} d\nu \left[\frac{k}{2Ha(t)}\right]^{-i\nu} \frac{\nu\Gamma(i\nu)}{f_+(\nu)} e^{-i\nu Hz'} J_{i\nu}\left[\frac{k}{Ha(t')}\right], \quad \frac{k}{Ha(t)} \ll 1. \quad (80)$$

This is the form of the Green's function that one would use to determine the behavior of Ω_b at late times. It is also interesting to consider the dynamics of modes which are in the superhorizon regime at the *beginning* of the de Sitter era: $k/Ha(t') \ll 1$. These are the modes which never actually enter the Hubble horizon. It is possible to explicitly evaluate the residues of \mathcal{G}_- in this case to obtain

$$G_-(t, t'; 0, z') \approx \Theta(\Delta t - \Delta z) \left\{ A_1 \left[\frac{a(t)}{a(t')} e^{-Hz'} \right]^{\epsilon/2} + A_2 \left[\frac{a(t)}{a(t')} e^{-Hz'} \right]^{3\epsilon/2 - 1/Hr_c} + \sum_{m=1}^{\infty} B_m \left[\frac{k^2 e^{Hz'}}{H^2 a(t) a(t')} \right]^m \right\}, \quad (81)$$

where A_1 , A_2 and B_m are functions of Hr_c . One can easily derive a similar expression for the advanced Green's function with coefficients C_1 , C_2 and D_m corresponding to the advanced modes in Table I.

The Green's function (81) reveals how scale-dependence outside the horizon can arise. The A_1 and A_2 contributions to G_- are independent of scale k/Ha . This is consistent with what we would expect in General Relativity for a mode that has $k/Ha \ll 1$ at the beginning of a de Sitter era: the evolution of the mode (as mediated by the Green's function) is expected to be independent of k . On the other hand, the contributions from the B_m modes carry an explicit k -dependence (this arises from the fact that $J_{i\nu}$ and $J_{-i\nu}$ are linearly dependent when $i\nu$ is an integer). This $(k/Ha)^2$ suppression is also familiar from General Relativity and represents the leading order correction to the gradient approximation. However, on the normal branch, when combined with more slowly growing A_1 and A_2 modes, the net growth rate of the metric fluctuations for superhorizon perturbations becomes k -dependent unlike in General Relativity.

We now turn our attention to finding a particular solution to the inhomogeneous equation (68) with the Δ source. In principle, one could use the retarded Green's function G_- to find $\varphi^{(p)}$, but it is easier to just solve for it directly in Eq. (68) by making a physically-motivated ansatz. In this calculation, we work in the $a \rightarrow \infty$ limit and retain only leading order terms. We make the following ‘‘outgoing-wave’’ ansatz for the bulk field:

$$\varphi^{(p)} \propto e^{i\nu H(t-z)}. \quad (82)$$

Substituting this into Eq. (68) and (69), we find that there are two values of ν consistent with $\Delta \neq 0$:

$$\nu = 3i/2 \text{ or } 7i/2. \quad (83)$$

The two distinct values of ν give rise to solutions for Δ and $\Omega_b^{(p)}$

$$\Delta(t) = \Delta_0 + \Delta_1 (a/a_*)^{-2}, \quad \Omega_b^{(p)} \equiv a^{3/2} \varphi_b^{(p)} = \frac{r_c \kappa_A^2 \rho a^3}{Hk^2} \begin{cases} \frac{\Delta_0}{3Hr_c - 1} + \frac{1}{2} \frac{a_*^2}{a^2} \frac{\Delta_1}{(5Hr_c - 1)}, & \epsilon = +1, \\ -2\Delta_0 + \frac{2}{3} \frac{a_*^2}{a^2} \frac{\Delta_1}{(2Hr_c - 1)}, & \epsilon = -1, \end{cases} \quad (84)$$

which confirms the scaling expectation [see Eq. (62)].

Having now determined how to obtain both homogeneous $\varphi^{(h)}$ and particular solutions $\varphi^{(p)}$ of Eq. (68) at late times, we can write down the following formulae for various quantities of cosmological interest

$$\Omega_b \approx \sum_i \Omega_0^{(i)} \left(\frac{a}{a_*} \right)^{p_i} + \Omega_b^{(p)}, \quad \Phi \approx \sum_i \Phi^{(i)} + \Phi^{(p)}, \quad \Psi \approx \sum_i \Psi^{(i)} + \Psi^{(p)}. \quad (85)$$

Here, p_i is the temporal scaling index of the i^{th} resonance of the *retarded* Green's function (i.e. the p -values for the $A_{1,2}$ and B_m modes listed in Table I), $\Omega_0^{(i)}$ are constants with dimension $(\text{length})^2$ related to the amplitudes (A_1, A_2, B_m) and recall a_* is the reference epoch at the beginning of the de Sitter phase [see Eq. (54)]. The resonant contributions to the metric potentials and comoving curvature perturbation are

$$\Phi^{(i)} = \frac{\Omega_0^{(i)} H^2 (p_i - 1)}{2a_* (2Hr_c \epsilon - 1)} \left(\frac{a}{a_*} \right)^{p_i - 1} \left[1 + \mathcal{O} \left(\frac{k^2}{H^2 a^2} \right) \right], \quad (86a)$$

$$\Psi^{(i)} = (p_i - 1) \Phi^{(i)} \left[1 + \mathcal{O} \left(\frac{k^2}{H^2 a^2} \right) \right]. \quad (86b)$$

For $p_i \neq 1$,

$$g_{\text{SH}}^{(i)} = \frac{p_i}{2 - p_i} \quad (87)$$

branch	matter era	A_1	A_2	B_1	particular mode
$\epsilon = +1$	$+9/(8Hr_c - 1)$	∞	$-\frac{3Hr_c - 1}{Hr_c - 1}$	$1/3$	0
$\epsilon = -1$	$-1/(2Hr_c + 1)$	n/a	$-1/(2Hr_c + 1)$	$1/3$	$-1/(2Hr_c + 1)$

TABLE II: The value of the quantity g in the superhorizon regime $k/Ha \ll 1$ in either branch.

for each mode on either branch. This scaling is in fact a direct consequence of $\zeta' = 0$ in Eq. (28) for $p_i \neq -2$.

On the self-accelerating branch with $\Omega_\Lambda = 0$, the growth index $p_i = 2$ for both A_1 and A_2 . This large growth rate makes them dominates over B and particular modes. In fact $g_{\text{SH}} \rightarrow \infty$, which explains its divergent behavior in Fig. 2. For the normal branch, the A_1 mode has $p_i = 1$ and thus no contribution to either Φ or Ψ . The k -independent solution that dominates is then A_2 but its growth index $p_i = -1/Hr_c$ is smaller than the B_1 mode $p_i = 1/2$. Thus the k -dependent B_1 mode dominates at late times for any finite k .

On the normal branch even the particular mode can be important. The particular contribution to the various quantities are given by

$$\Phi^{(\text{p})} = \frac{\kappa_4^2 \rho a^2 Hr_c}{k^2} \begin{cases} +\frac{3}{2} \frac{\Delta_0}{3Hr_c - 1}, & \epsilon = +1, \\ -\frac{1}{3} \left(\frac{k}{Ha}\right)^2 \frac{\Delta_0}{2Hr_c + 1} + \left(\frac{a_*}{a}\right)^2 \frac{2Hr_c \Delta_1}{4H^2 r_c^2 - 1}, & \epsilon = -1, \end{cases} \quad (88a)$$

$$\Psi^{(\text{p})} = \frac{\kappa_4^2 \rho a^2 Hr_c}{k^2} \begin{cases} -\frac{3}{2} \frac{\Delta_0}{3Hr_c - 1}, & \epsilon = +1, \\ +\frac{2}{3} \left(\frac{k}{Ha}\right)^2 \frac{\Delta_0}{2Hr_c + 1} - \left(\frac{a_*}{a}\right)^2 \frac{2(Hr_c + 1)\Delta_1}{4H^2 r_c^2 - 1}, & \epsilon = -1. \end{cases} \quad (88b)$$

Note that for the normal branch the leading order Δ_0 term vanishes and contributions are suppressed by $(k/Ha)^2$. Hence for modes that are outside of the horizon at the de Sitter transition $(k/Ha_*)^2 \ll 1$ we expect that the main contribution from the particular mode comes from Δ_1 . Under these assumptions the leading order scalings give

$$g_{\text{SH}}^{(\text{p})} = \begin{cases} 0, & \epsilon = +1 \\ -\frac{1}{2Hr_c + 1}, & \epsilon = -1. \end{cases} \quad (89)$$

For the normal branch, the growth index $p^{(\text{p})} = -2$ and hence can become the leading order k -independent term if $-1/Hr_c < -2$. However the value of g_{SH} remains the same as for the A_2 mode and is in fact the same as the matter dominated scaling. Therefore on the normal branch, the leading order k -independent term can be modeled as $g_{\text{SH}} = -1/(2Hr_c + 1)$ regardless of which of those modes actually dominates the solution. This simplification was employed by [9] to model perturbation evolution to the present epoch and obtain observational constraints on $H_0 r_c$.

In Table II, we list the values of g_{SH} associated with each of the modes appearing in Eqs. (86) and (88), as well as the values of g_{SH} in matter domination from §IV B. These relations supplemented by the quasistatic analysis complete the analytic description.

V. FITTING FUNCTIONS

Given the analytic description of perturbations in the matter and de Sitter epochs above and below the horizon in §IV, we now devise global fitting functions for the perturbation evolution that bridge the transition and apply across all scales and epochs. We focus primarily on the normal branch but also test existing fits for the self-accelerating branch that have been used to show its predictions are in conflict with CMB data [5, 15].

A. Normal Branch

As discussed in §II C, once $g = (\Phi + \Psi)/(\Phi - \Psi)$ is determined, solving for the metric itself is a simple matter of applying conservation of the comoving curvature on large scales or the modified Poisson equation on small scales. Moreover $g = 0$ for General Relativity without anisotropic stress sources and an accurate quantification of its value in DGP is important for observational test of gravity.

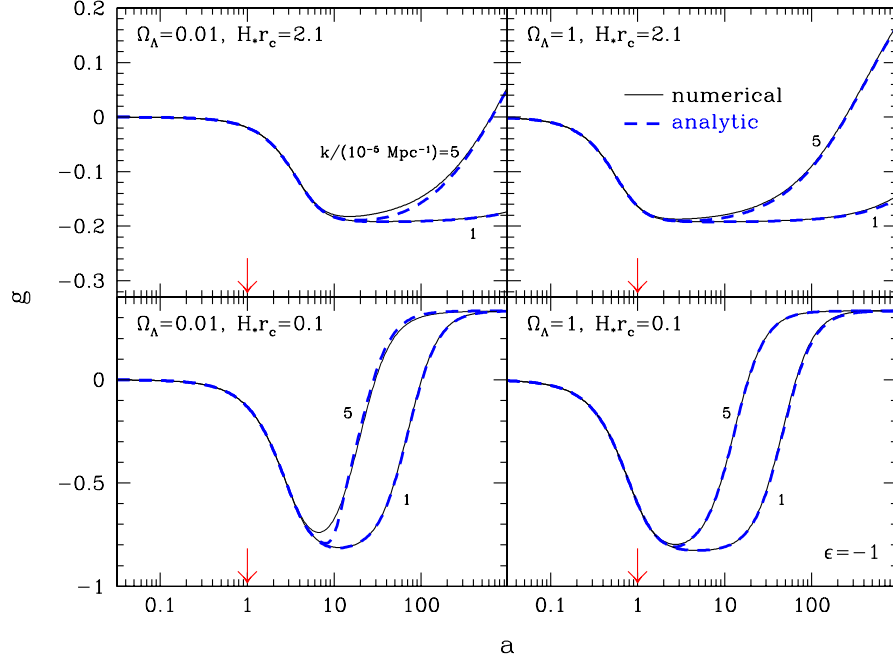


FIG. 4: Metric ratio g for purely superhorizon modes for normal branch ($\epsilon = -1$). Analytic fit from Eq. (93) (dashed lines) match the numerical CI calculation well for a wide range of parameters. Note that even on superhorizon scales g is scale dependent due to the relative importance of the A , B , and particular modes. The current epoch is denoted by the arrow.

We begin by describing the superhorizon behavior. As shown in the previous section, there are several modes of importance during and after the transition to a de Sitter expansion. Although the growth rate of all modes are independent of scale above the horizon, their initial amplitudes are not. In particular, after the de Sitter transition at a_* where $H(a \rightarrow \infty) = H_* = H(a_*)/\sqrt{2}$ [see Eqs. (53) and (54)], there are scale-free modes and modes that come from higher order terms in the gradient approximation that are suppressed by powers of (k/H_*a_*) . The leading order mode B_1 has a faster growth rate and though initially suppressed will eventually dominate on all scales [see Eq. (81)]. B_1 requires $g = 1/3$ whereas for the scale free A resonant and density-driven particular modes $g = -1/(2Hr_c + 1)$.

Given these relations and the growth rates of the three modes, we seek to describe the superhorizon behavior as

$$g_{\text{SH}}(a, k) = \frac{(k/H_*a_*)^2 - [K_1(a/a_*)^{-1/2-1/H(a)r_c} + K_2(a/a_*)^{-5/2}]}{3(k/H_*a_*)^2 + [2H(a)r_c + 1][K_1(a/a_*)^{-1/2-1/H(a)r_c} + K_2(a/a_*)^{-5/2}]}. \quad (90)$$

With

$$K_1 = 13.2 \left(\frac{H_*r_c + 1}{H_*r_c} \right)^2, \quad (91a)$$

$$K_2 = 30.9(2H_*r_c + 1)^2, \quad (91b)$$

we are able to fit the results of the CI numerical solution very well from matter domination through de Sitter expansion for 240 models with $0.1 < H_*r_c < 10$, $0.01 < \Omega_\Lambda < 1$, and $k/H_*a_* \lesssim 1$. Examples of the fit are shown in Fig. 4.

The subhorizon form of g approaches the quasistatic behavior at $k/Ha \gg 1$

$$g_{\text{QS}}(a) = -\frac{1}{3} \frac{1}{1 - 2\epsilon Hr_c(1 + H'/3H)}. \quad (92)$$

Note that in the de Sitter epoch, modes exit the horizon. In choosing a functional form for mediating the transition it is useful to note that the first order predicted solution is $g = g_{\text{QS}}(1 + \mathcal{O}(Ha/k))$ from §IV A. Unfortunately it does not suffice to simply match a first order correction to the superhorizon modes at horizon crossing. Instead we find that the following interpolation

$$g(a, k) = \frac{g_{\text{SH}} + g_{\text{QS}}K_3}{1 + K_3} \quad (93)$$

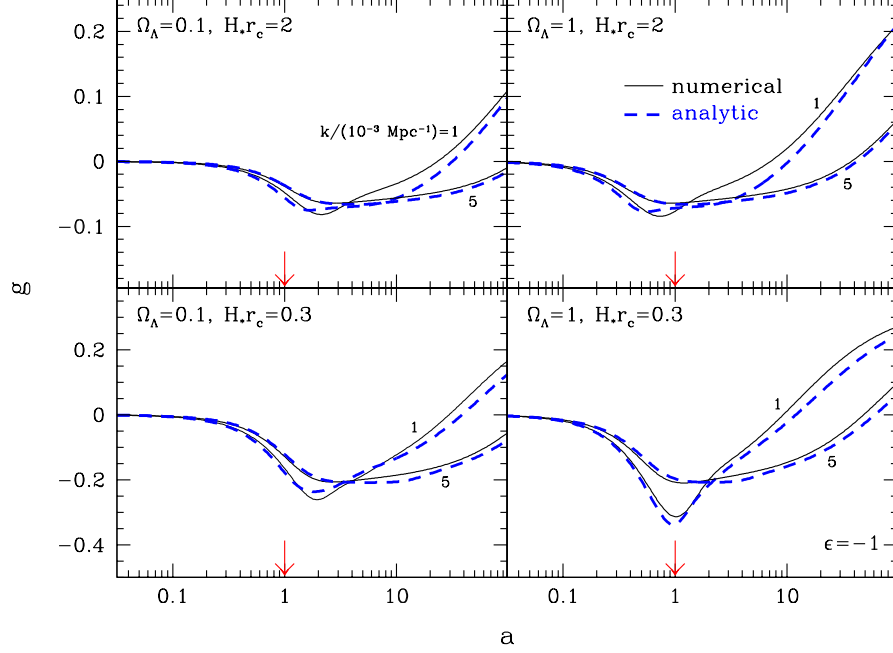


FIG. 5: Metric ratio g for modes that are currently horizon and sub-horizon scale for the normal branch ($\epsilon = -1$). Analytic fit from Eq. (93) (dashed lines) match the qualitative features of the numerical CI calculation across the full range of parameters. In particular, the fit is designed to approach the correct behavior for $k/Ha \ll 1$, $k/Ha \gg 1$ and $a/a_* \gg 1$. Note that currently subhorizon modes exit the horizon in the future de Sitter epoch. The current epoch is denoted by the arrow.

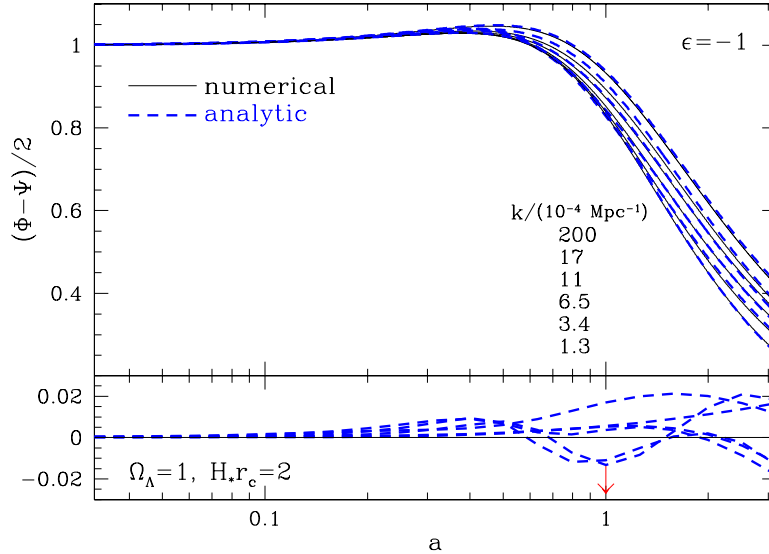


FIG. 6: Observable lensing potential $(\Phi - \Psi)/2$ on normal branch ($\epsilon = -1$). Analytic fit to the metric ratio g compared with the numerical CI calculation (top panel). In spite of imperfections in the g -fit for currently horizon scale modes, fractional differences (bottom panel) are $< 2\%$ for $a < 1$. The current epoch is denoted by the arrow.

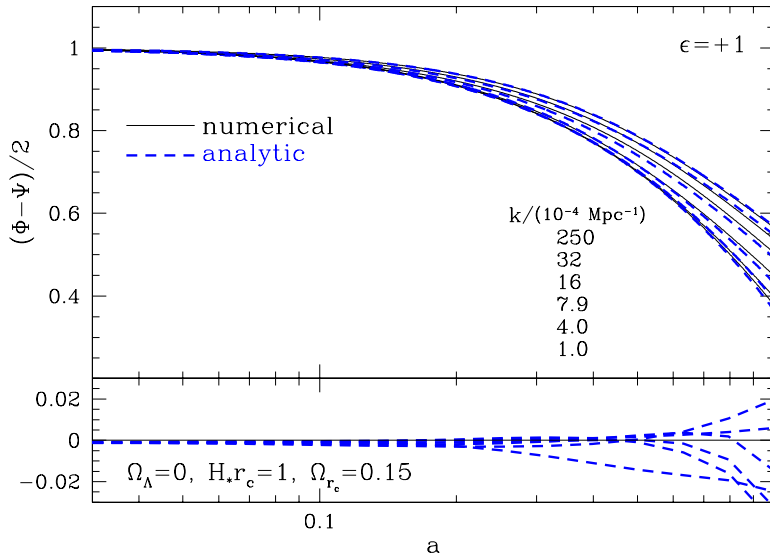


FIG. 7: Observable lensing potential $(\Phi - \Psi)/2$ on self-accelerating branch ($\epsilon = +1$). Analytic fit to the metric ratio g compared with the numerical CI calculation (top panel). Fractional differences in the observable potential are $< 2\%$ for $a < 1$ (bottom panel).

with

$$K_3 = \left(0.18 \frac{k}{Ha}\right)^6 \left[1 + \frac{(8.1a/a_*)^5}{3^5 + (k/H_* a_*)^5} (3H_* r_c + 1)\right] \quad (94)$$

better describes the $k/Ha \sim 1$ horizon-crossing regime while providing a negligible mismatch in the $k/Ha \gg 1$ limit. Note that for $k/Ha \gg 1$ and $a/a_* \gg 1$, the first order correction of Eq. (39) gives $(g - g_{\text{QS}})/g_{\text{QS}} = -2(H_* a/k)$ whereas the fit gives $(g - g_{\text{QS}})/g_{\text{QS}} = -1.7(H_* a/k)(1 + H_* r_c)/(3 + H_* r_c)$. That the functional form in k is correct and the $H_* r_c$ corrections are bounded from $1/3$ to 1 ensures that we do not have a runaway mismatch for any set of parameters.

As shown in Fig. 5, the fit captures the qualitative features of the numerical solution, including the asymptotic behavior at $a/a_* \gg 1$. Although imperfect, the fit suffices for observational constraint purposes. In Fig. 6, we show the performance of the fit for the metric combination involved in gravitational lensing and gravitational redshifts $(\Phi - \Psi)/2$. Here we have set the transition scale between constant comoving curvature and Poisson-like behavior to $c_\Gamma = 0.15$ [15]. Note that fractional errors are below 2% for $a < 1$ for all scales.

B. Self-Accelerating Branch

Similar fitting functions for the self-accelerating branch were given in [15] for $a < 1$ and $\Omega_\Lambda = 0$. For superhorizon scales

$$g_{\text{SH}}(a) = \frac{9}{8H_* r_c - 1} \left(1 + \frac{0.51}{H_* r_c - 1.08}\right).$$

and the interpolation factor in Eq. (93) is given by $K_3 = (0.14k/Ha)^3$ with the transition scale set by $c_\Gamma = 1$. In Fig. 7, we compare the predicted lensing potential to the numerical integration up to the present epoch. Given that we have shown that g_{SH} actually diverges deep in the de Sitter epoch (see Tab. II and Fig. 2), it is not surprising the errors in the fit increase toward the current epoch. Still those errors are $\lesssim 2\%$ at the time scales relevant for observational constraints. This should be compared with the much larger change in the potential of a factor of ~ 2 .

VI. DISCUSSION

We have provided analytic solutions for the linear evolution of metric perturbations in the DGP modified gravity models in various regimes where scaling and Green's function techniques are applicable. We have elucidated the nature of the coordinate singularities and initial data in the bulk as well as their effect on perturbation evolution on the brane.

Interestingly, even on superhorizon scales, the evolution of metric perturbations is no longer necessarily scale free. In the late-time de Sitter phase on the normal branch, several resonant modes are excited with different growth rates and amplitudes. The epoch at which the fastest growing mode dominates depends on scale. On the other hand, for reasonable parameters where the de-Sitter phase has only recently been entered these complexities are mainly manifest in the future and do not affect observational tests [9].

Based on these analytic solutions, we have devised convenient fitting functions for the evolution that bridge the various spatial and temporal regimes for the normal branch. These forms are valid for essentially the whole range of parameter space and have been tested against numerical integration of 240 models spanning $0.1 < H_* r_c < 10$, $0.01 < \Omega_\Lambda < 1$ with multiple k -modes for each. For the self-accelerating branch we have verified the accuracy of existing fitting formulae for the cases of interest [15].

Compared with a direct numerical integration of the bulk equations, these forms are accurate at the percent level which is sufficient for current and upcoming observational tests of the DGP scenario from the cosmic microwave background and weak gravitational lensing.

Acknowledgments: We thank Y.S. Song for collaboration during the initial phases of this project. SSS is supported by NSERC of Canada. WH was supported by the KICP under NSF contract PHY-0114422, the DOE contract DE-FG02-90ER-40560 and the Packard Foundation.

-
- [1] G. R. Dvali, G. Gabadadze and M. Porrati, Phys. Lett. **B485**, 208 (2000), [arXiv:hep-th/0005016].
 - [2] C. Deffayet, Phys. Lett. **B502**, 199 (2001), [arXiv:hep-th/0010186].
 - [3] I. Sawicki, Y.-S. Song and W. Hu, Phys. Rev. **D75**, 064002 (2007), [arXiv:astro-ph/0606285].
 - [4] Y.-S. Song, I. Sawicki and W. Hu, Phys. Rev. **D75**, 064003 (2007), [arXiv:astro-ph/0606286].
 - [5] W. Fang *et al.*, Phys. Rev. **D78**, 103509 (2008), [arXiv:0808.2208].
 - [6] A. Cardoso, K. Koyama, S. S. Seahra and F. P. Silva, Phys. Rev. **D77**, 083512 (2008), [arXiv:0711.2563].
 - [7] K. Koyama, Class. Quant. Grav. **24**, R231 (2007), [arXiv:0709.2399].
 - [8] Y.-S. Song, Phys. Rev. **D77**, 124031 (2008), [arXiv:0711.2513].
 - [9] L. Lombriser, W. Hu, W. Fang and U. Seljak, Phys. Rev. **D80**, 063536 (2009), [arXiv:0905.1112], used preliminary results from this work with $g_{SH} = -1/(2Hr_c + 1)$ for normal branch.
 - [10] T. Shiromizu, K.-i. Maeda and M. Sasaki, Phys. Rev. **D62**, 024012 (2000), [arXiv:gr-qc/9910076].
 - [11] K.-i. Maeda, S. Mizuno and T. Torii, Phys. Rev. **D68**, 024033 (2003), [arXiv:gr-qc/0303039].
 - [12] C. Deffayet, Phys. Lett. **B502**, 199 (2001), [arXiv:hep-th/0010186].
 - [13] S. Mukohyama, Phys. Rev. **D62**, 084015 (2000), [arXiv:hep-th/0004067].
 - [14] C. Deffayet, Phys. Rev. **D66**, 103504 (2002), [arXiv:hep-th/0205084].
 - [15] W. Hu and I. Sawicki, Phys. Rev. **D76**, 104043 (2007), [arXiv:0708.1190].
 - [16] K. Koyama and R. Maartens, JCAP **0601**, 016 (2006), [arXiv:astro-ph/0511634].
 - [17] A. Lue, R. Scoccimarro and G. D. Starkman, Phys. Rev. **D69**, 124015 (2004), [arXiv:astro-ph/0401515].
 - [18] W. Fang, W. Hu and A. Lewis, Phys. Rev. **D78**, 087303 (2008), [arXiv:0808.3125], see also <http://camb.info/ppf>.
 - [19] S. S. Seahra, Phys. Rev. **D74**, 044010 (2006), [arXiv:hep-th/0602194].
 - [20] M. A. Amin, R. V. Wagoner and R. D. Blandford, Mon.Not.Roy.Astron.Soc. (2007), [arXiv:0708.1793].